Ann. Geophys. Discuss., https://doi.org/10.5194/angeo-2019-45
Manuscript under review for journal Ann. Geophys.
Discussion started: 25 March 2019

Annales Geophysicae Discussions
Open Access
EGU

,

Global Climatology of Equatorial Plasma Bubbles based on GPS Radio Occultation from FormoSat-3/COSMIC

Ankur Kepkar[1,2], Christina Arras[2], Jens Wickert[1,2], Harald Schuh[1,2], Mahdi Alizadeh[1,3], and Lung-Chih Tsai[4]

[1]Technische Universität Berlin, Germany
[2]German Research Centre for Geosciences GFZ, Potsdam, Germany
[3] K.N. Toosi University of Technology, Tehran, Iran
[4]National Central University, Chung-Li, Taiwan

Correspondence: Ankur Kepkar (kepkar@gfz-potsdam.de)

Abstract. The emerging technique of GPS Radio Occultation has been used to detect the ionospheric irregularities prominent in the F-region known as equatorial plasma bubbles. The plasma bubbles are characterized by depreciated regions of electron density. For investigating the plasma bubbles, a nine-year (2008-2016) long time series of signal-to-noise ratio data are used from the vertical GPS radio occultation profiles. The variation in the signal-to-noise ratio of the GPS signals can be linked to vertical changes in the electron density profiles that mainly occur in line with the irregularities in the Earth's ionosphere. The analysis revealed that the F-region irregularities, associated with plasma bubbles occur mainly post sunset close to Earth's geomagnetic equator. Dependence on the solar cycle as well as distinctive seasonal variation is observed when analyzed for different years. In contrast to the other ionospheric remote sensing methods, GPS Radio Occultation technique uniquely personifies the activity of the plasma bubbles based on altitude resolution on a global scale.

1 Introduction

The GPS (Global Positioning System) signals operating at radio frequencies provide extensive scope for navigation, communication and remote sensing. However due to various propagation deterrents, the accuracy of the GPS signals is curbed causing serious implications on its applications. One of the error sources arises during propagation of the signals through the ionosphere, which is embedded in parts of mesosphere and thermosphere. The Earth's ionosphere is a dispersive medium consisting of free charge carriers, extending at an altitude range between $60\,km$ to about $1000\,km$. Among different vertical regions of the ionosphere, the F region consists of high electron density and offers highly dynamic environment. Due to its volatility, the radio signals undergo scintillations mainly caused by underlying ionospheric irregularities. Consequently, the

Ann. Geophys. Discuss., https://doi.org/10.5194/angeo-2019-45
Manuscript under review for journal Ann. Geophys.
Discussion started: 25 March 2019

Annales Geophysicae Discussions

incoming radio waves traversing through an ionized medium are received as degenerated signals. The scintillated signals are, therefore, used to understand and exploit the various possibilities for ionospheric disturbances which cause signal degradation.

The focus of this research relies on the ionospheric irregularity known as Equatorial Plasma Bubbles (EPBs). This irregularity causes amplitude as well as phase scintillations on the radio signals used for various GPS applications. The plasma bubbles, prominent in the low latitudinal regions, are characterized by sharp depletion in the electron density (Fejer and Kelley, 1980). The EPBs instigated by plasma irregularities are also known by its generic name as Equatorial Spread F (ESF), which is perceived as diffused echoes from ionosonde readings (Booker and Wells, 1938). Apart from scintillations on the radio signal, this irregularity manifests themselves as plume like structure in the range time intensity images from incoherent scatter radar (Kudeki and Bhattacharyya, 1999) and intensity bite-outs in airglow measurements (Sahai et al., 2000). Through theories, related to seeding of plasma instabilities, it was predicated that Rayleigh-Taylor instabilities caused plasma bubbles to evolve, which eventually advanced from the depleted bottomside to higher density topmost F-region of the ionosphere (Woodman, 2009). Apart from this seeding theory, recent developments on gravity waves, though in the elementary stage, are being proposed for theories related to seeding of plasma instabilities (Taori et al., 2011). The EPBs are a night time phenomena influenced by solar activity (Carter et al., 2013). The plasma bubbles were initially identified with in-situ measurements by Hanson and Sanatani (1973) and later confirmed by McClure et al. (1977). Ever since, there has been considerable amount of research conducted on EPBs using ground based as well as in-situ measurements. Moreover, the satellite measurements provided the opportunity of significant global coverage over ground based measurements, since the latter are fixed at particular geographical coordinates. In this paper, the GPS Radio Occultation (GPS-RO) technique is adopted to produce climatological synopsis of EPBs providing significant altitudinal variations in addition to spatial coverage.

The GPS-RO is a space based technique, which operates on high-low satellite satellite tracking (HL-SST) mode (Wickert et al., 2009). It is mainly based on tracking the radio signals from the GPS satellites as they penetrate through the Earth's atmosphere, causing the signal to bend while crossing it. The fundamental observable obtained from bending of the signal due to refraction is the bending angle, which is measured as an additional Doppler shift for accurate frequency and orbit geometry measurements (Kursinski et al., 1997). The parameters, including the electron density profiles in the ionosphere are simply obtained using the onion peeling algorithm (Lei et al., 2007). In the stratosphere and troposphere, temperature and pressure profiles are obtained additionally through refractivity profiles (Wickert et al., 2002). GPS-RO has been increasingly used for various remote sensing applications, since it does not require calibration and offers extensive global coverage, high vertical resolution profiles, long term stability and operates under all weather conditions (Rocken et al., 1997). In the past, various LEO (Low Earth Orbiter) mission contributed towards radio occultation operations such as GPS/MET (GPS/METeorology), CHAMP (CHAllenging Minisatellite Payload), GRACE (GRAvity recovery and Climate Experiment), FormoSat-3/COSMIC (Formosa Satellite -3/Constellation Observing System for Meteorology, Ionosphere and Climate) (Wickert et al., 2009; Arras et al., 2010).

Ann. Geophys. Discuss., https://doi.org/10.5194/angeo-2019-45
Manuscript under review for journal Ann. Geophys.
Discussion started: 25 March 2019

2 Data analysis

The GPS-RO measurements for constructing a nine-year synoptic climatology of EPBs were obtained from FormoSat-3/COSMIC. This LEO mission consisting of six satellites constellation has been providing comprehensive measurements of around 2,000 profiles per day (Anthes et al., 2008). However, after orbiting for more than 12 years and providing continuous measurements, the number of RO profiles have nearly reduced to approximately 10% since 2016. This is because, five out of six satellites became non-functional due to various system failures and the remaining one is only operational under degraded mode (Chu et al., 2018).

2.1 Data availability

The FormoSat-3/COSMIC satellite measurements provide near real-time RO observations (Anthes et al., 2008). The data is available from the web portal of COSMIC Data Analysis and Archival Center (CDAAC) database, which is managed by University Corporation for Atmospheric Research (UCAR), Colorado, United States of America. The files from the CDAAC database are available in various formats including Bernese RINEX (BINEX) for GPS data and NetCDF for higher level products. Around 5 millions of higher level data products, belonging to *level 1* RO profiles were downloaded on a year-wise basis from 2008-2016. The operational data, namely the *ionPhs* (*ion*ospheric excess *Ph*ases for generating ionospheric profiles) data under *level 1b* products were used for realizing the primary interest of this work. It was articulated that amplitude variation on the RO signal had a direct influence on the ionospheric characteristics along with space weather condition (Wickert et al., 2004). Therefore for identifying ionospheric irregularities, raw SNR RO profiles are considered over electron density profiles, since the amplitude measurements are readily available and no further data treatment is required. Moreover, it was learned from RO profiles that sudden depletion in the electron density has reciprocity of weakened SNR on the GPS signal, which in turn translated into strong scintillations as illustrated in Fig. 1.

2.1.1 Derivation of amplitude scintillation index

The RO measurements obtained from FormoSat-3/COSMIC, essentially scan the atmosphere in two frequencies. The upper atmosphere is scanned with $1\,Hz$ frequency with altitude resolution of approximately $2\,km$ for an altitude range from $50\,km$ above Earth's surface up to the orbital height of LEO. Whereas the neutral atmosphere having upper altitude limit of around $130\,km$ is sampled at $50\,Hz$ having an altitude resolution of approximately $50\,m$ (Arras et al., 2008). To single out plasma bubbles resulting from ionospheric instabilities, GPS L1 amplitude measurements were opted over L2 measurements. Since the frequency of the L2 signal is close to the critical frequency of the ionosphere, the L2 signal becomes more susceptible to ionospheric irregularities, which sometimes result in loss of lock on the receiver and signal fading (Ahmed et al., 2018). On the other hand, L1 signal is easier to decrypt and shows strong signal characteristics when compared to L2 signals. Apart from

Ann. Geophys. Discuss., https://doi.org/10.5194/angeo-2019-45
Manuscript under review for journal Ann. Geophys.
Discussion started: 25 March 2019

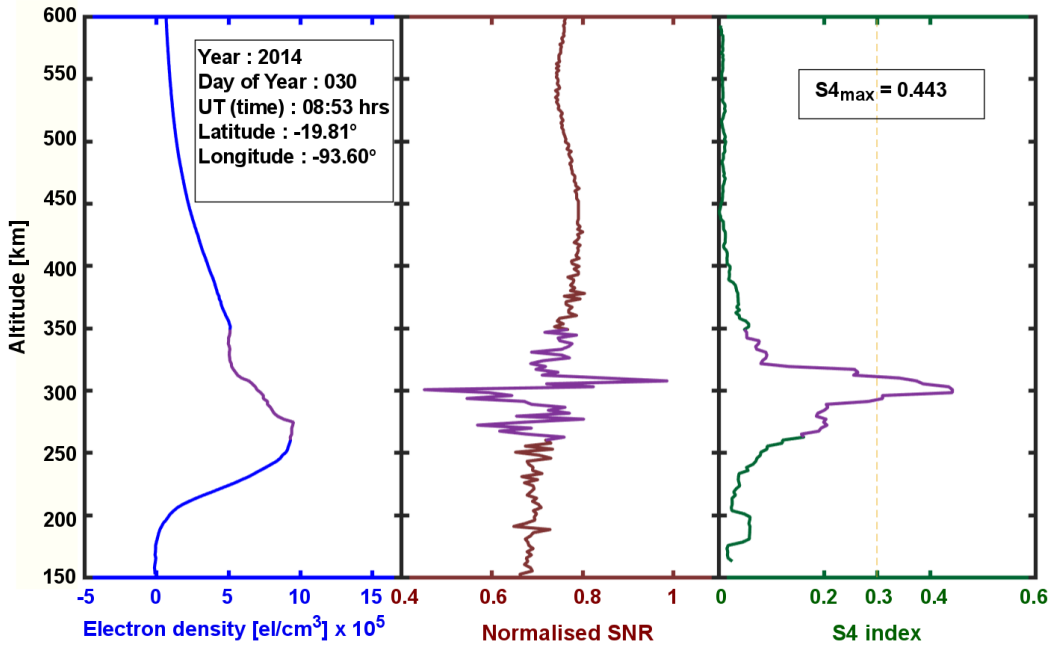

Figure 1. Electron density profile (ionPrf product) in conjunction with normalized SNR and derived S4 index (ionPhs product). The purple color line in the plot shows depletion in electron density and corresponding fluctuations in normalized SNR profile and high index values in the S4 plot.

SNR of L1 ($1575.42\,MHz$) signals, other corresponding attributes such as Universal Time, altitude, latitude and longitude are extracted from the data product and amplitude scintillation index is derived as described by Syndergaard (2006) in Eq. 1.

$$S4max9sec = \frac{\sqrt{\left\langle \left(I - \left\langle \bar{I} \right\rangle \right)^2 \right\rangle}}{\left\langle \bar{I} \right\rangle} \tag{1}$$

where $S4max9sec$ denotes the amplitude scintillations over 9 seconds interval, *I* is the square of the Signal-to-Noise (SNR) ratio of L1 GPS signal, and the brackets $\langle\rangle$ stand for average taken over nine seconds. A low pass filter is applied to the time series of these values to obtain a new average of the intensity $\langle \bar{I} \rangle$. This new intensity value can be used for deriving S4 index as a more corrected mean value. Within this work, $S4max9sec$ is computed from raw SNR L1 data and its corresponding mean values of Universal Time, local time, latitude, longitude and altitude of each profile is taken into consideration. A simple representation of $S4max9sec$ versus local time during the year 2014 is depicted in Fig. 2 showing scattered scintillation

Ann. Geophys. Discuss., https://doi.org/10.5194/angeo-2019-45
Manuscript under review for journal Ann. Geophys.
Discussion started: 25 March 2019

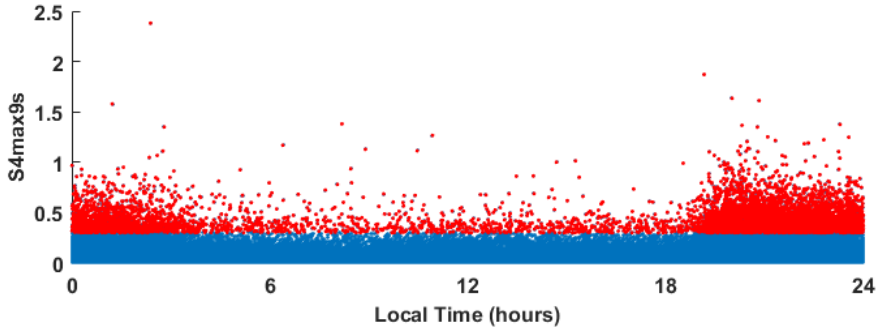

Figure 2. Plot of $S4max9sec$ as a function of local time (LT) during 2014. The blue dots represent the scintillation index less than 0.3, whereas strong scintillations are represented by the red dots having S4 index larger than 0.3.

values caused by different gradients of electron density. Additionally, it also highlights low S4 index values during day and high scintillation values during night resulting from plasma instabilities caused by rapid depletion of E-region post sunset. During 2014 altogether about 0.5 million profiles were retrieved, out of which only 6,130 profiles were classified as strong scintillating events resulting from plasma bubbles. Thus, around 1.2% profiles were encountered globally, which included strong scintillation events, produced, as a result of EPBs.

Our study exclusively focuses on scintillation events, which are primarily based on S4 index. We classify scintillations based on different values as presented in Table 1. Hereafter $S4max9sec$ index will be referred as S4 index. Within this work, S4 index values greater than 0.3 are used to quantify the strong scintillation events caused by plasma bubbles (Seif et al., 2017).

***S4* values**	**scintillation category**	**occurrence (2014)**
$S4 \geq 1.0$	high	0.02%
$0.3 < S4 < 1$	moderate	1.19 %
$S4 \leq 0.3$	low	98.79%

Table 1. Categorization of S4 index intensity.

3 Results

The most comprehensive time series from FormoSat-3/COSMIC mission is exploited for the scientific study of plasma bubbles occurring in the equatorial region during 2008-2016. The advantage of using satellite based GPS-RO technique is that, it uniquely allows to quasi-vertically scan from the topside of the ionosphere to the bottomside and further down in the neutral atmosphere. Whereas other techniques such as satellite based in-situ measurements explore prevailing ionospheric condition along its orbital track. Therefore by employing the GPS-RO technique, a distinct attempt was made to quantify the occur-

Ann. Geophys. Discuss., https://doi.org/10.5194/angeo-2019-45
Manuscript under review for journal Ann. Geophys.
Discussion started: 25 March 2019

rence of EPBs both globally and altitudinally based on amplitude scintillation index. In order to centralize this study on the equatorial region, the latitudinal extent is filtered for 50° N/S. By doing this, polar scintillation events are excluded, thus focusing explicitly on the equatorial scintillation events. The EPBs identified in the following contour plots show low S4 values altogether, since they are derived as the mean on all RO S4 profiles. This further explains the influence of low scintillation category events, which are in high percentage as compared to moderate to high scintillation category as revealed in Table 1. In the following sections, different visual contours as well as graphical representations will be introduced to envisage various plausible depictions of EPBs.

3.1 Global distribution of EPBs

From SNR, S4 index is derived along with its corresponding attributes for understanding the occurrence of plasma bubbles. By producing maps for global distribution based on grid resolution of 20° in longitude and 5° in latitude, the spatial characteristics of the ionospheric irregularity is observed in Fig. 3. By performing such analysis, different distinctive aspects in occurrences can be noticed. One such peculiarity that can be perceived is, that the EPBs invariably follows the course of geomagnetic equator. For a general description of occurrence of plasma bubbles along the geomagnetic equator, the reader can refer to Kil (2015). The overall magnitude of plasma bubbles seem to drop during the year 2009. On the other hand, from 2010 there is an increase in the existence of high scintillation events with the highest magnitude reaching during 2014. The existence of the EPBs with respect to different years shows convincing accordance and relation to the solar cycle. The different conditions of solar cycle 24 explains that the solar minimum and solar maximum were observed during the year 2009 and 2014, respectively. Investigation on the dependency of occurrence of plasma bubbles in response to the conditions of solar cycle provides a general agreement with the results presented by Chu et al. (2005). In addition, F-region scintillations with respect to different regional sectors along with local time occurrence, magnetic and solar activity has been covered by Tsai et al. (2017) through means of GPS-RO data . During the solar minimum years, most of the EPBs are concentrated in the American sectors within the South Atlantic anomaly region. One of the reason is the magnetospheric particle precipitation, which had a compelling effect on the equatorial electrodynamics related to plasma irregularities (Burke et al., 2004). On the contrary, as we proceed towards the solar maximum years, the occurrence of EPBs seems to be dominant in the Atlantic-African sectors having strong magnitude. The reason behind such occurrence is unclear, due to inadequate research in the past over the region. However it is likely understood that either convection driven gravity waves or the localized charged dust particles arising from the dust storms which are prominent over the tropical region of Sahara desert could have a probable linkage to the occurrence of plasma irregularities over the Atlantic-African region (Yizengaw et al., 2011, 2013).

3.2 Local time occurrence

Different studies carried out related to plasma bubbles from ground as well as from in-situ measurements demonstrate the occurrence of plasma bubbles post-sunset corresponding to its geographical local time (Woodman and La Hoz, 1976; Whalen, 1997; Sahai et al., 2000; Gentile et al., 2006). Since the FormoSat-3/COSMIC satellites fly in non-sun synchronous orbits, it provides the possibility of analyzing plasma bubbles based on the local time. For manifestation, a contour representation of

Ann. Geophys. Discuss., https://doi.org/10.5194/angeo-2019-45
Manuscript under review for journal Ann. Geophys.
Discussion started: 25 March 2019

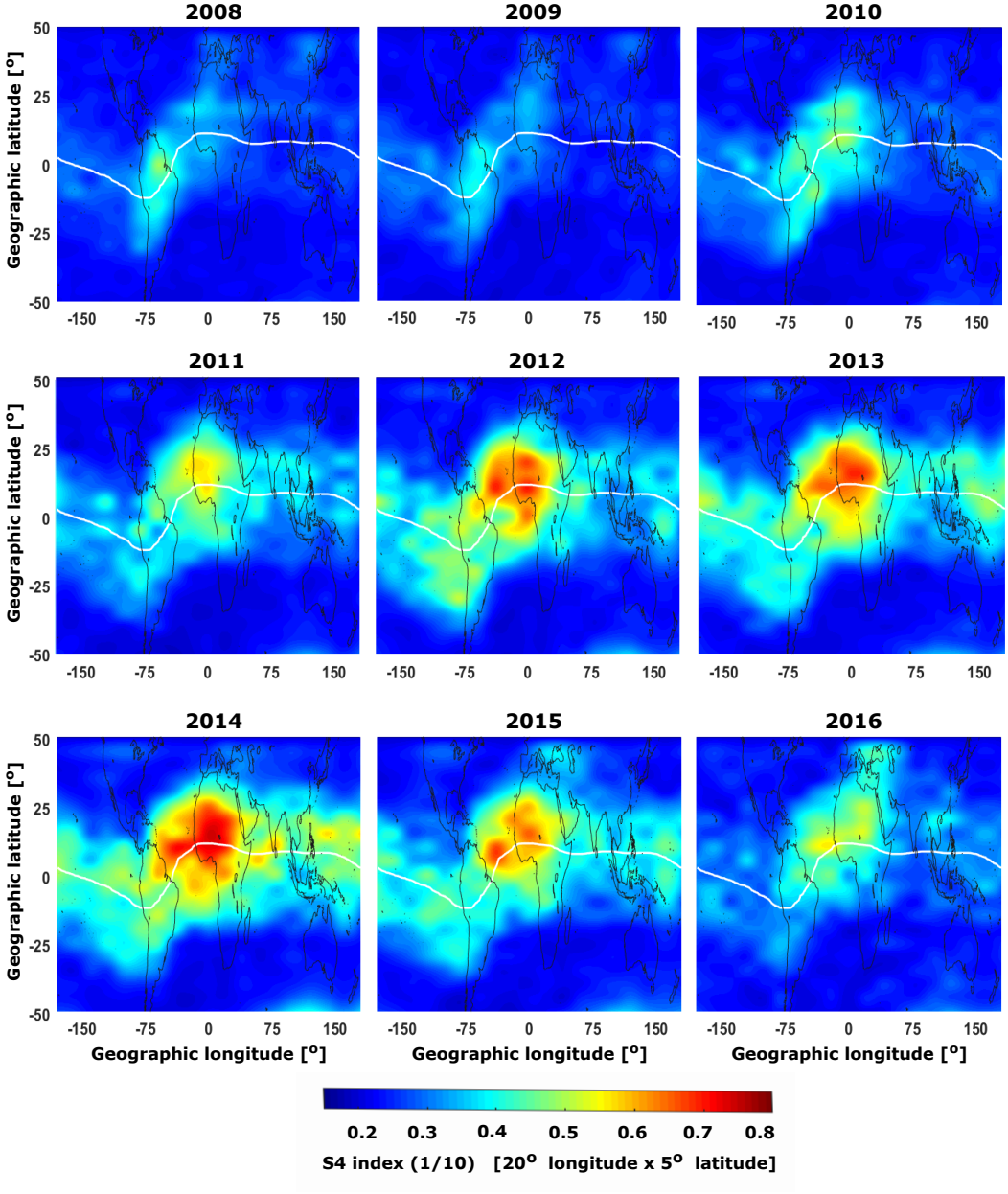

Figure 3. Plot of geographical latitude [°] v/s geographical longitude [°] of EPBs from 2007 to 2016 based on S4 index values. The white solid line depicts the geomagnetic equator.

local time during the year 2014 is illustrated in Fig. 4. The plot is based on local time and latitude measurements binned in a 1 hour $\times$ 5° grid resolution. The plots show clear evidence of EPBs developing roughly after 19:00 LT rightly after the E-region conductivity shorts out, causing rapid plasma depletion similar to that affirmed by Stolle et al. (2006). In addition, during solar

Ann. Geophys. Discuss., https://doi.org/10.5194/angeo-2019-45
Manuscript under review for journal Ann. Geophys.
Discussion started: 25 March 2019

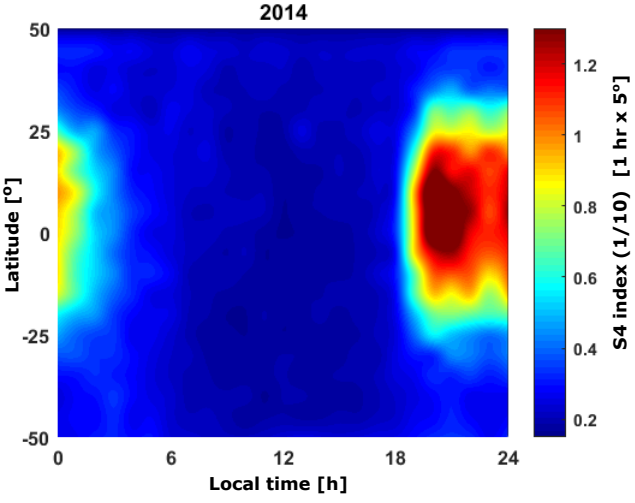

Figure 4. Latitude and local time dependence of the EPBs based on S4 index values represented in the form of geographical latitude v/s local time plots during 2014.

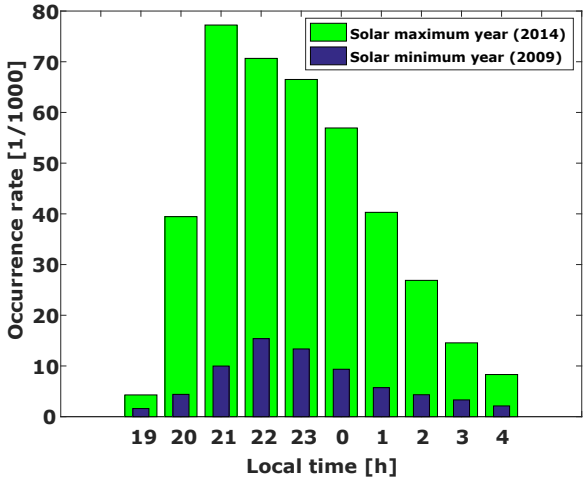

Figure 5. Occurrence of EPBs based on local time during solar minimum year (2009) and solar maximum year (2014) respectively.

maximum year (2014), the magnitude of these events culminated around 21:00 LT as portrayed in Fig. 5. Whereas during the solar minimum period (2009), the peak magnitude was found to occur around 22:00 LT identical to the results presented by Xiong et al. (2010) from CHAMP and GRACE in-situ measurements. Thus it is apparent that the events encountered using GPS-RO, fall in-line with the plasma bubble events discovered by previously used different probing techniques.

Ann. Geophys. Discuss., https://doi.org/10.5194/angeo-2019-45
Manuscript under review for journal Ann. Geophys.
Discussion started: 25 March 2019

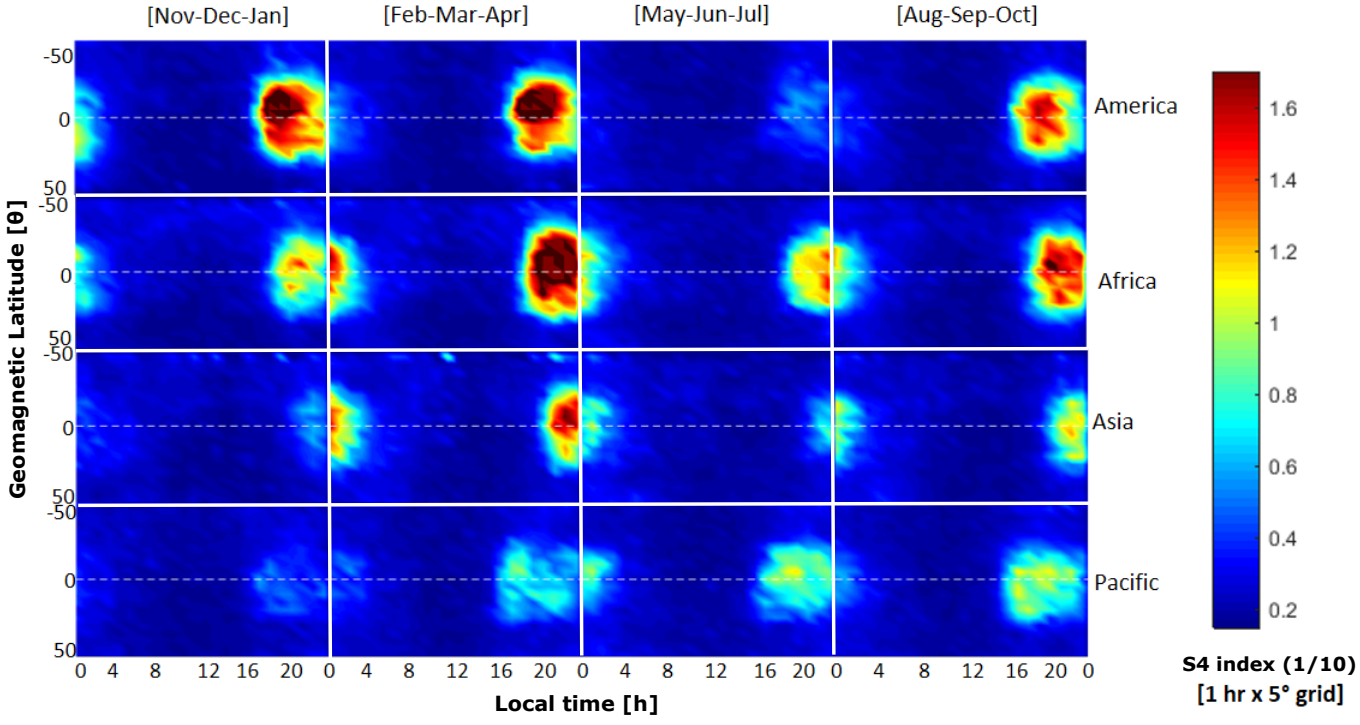

Figure 6. EPBs occurrence during the years 2012-2016 for different longitude sectors (regions) based on three month intervals (season). White dashed line represent geomagnetic dip equator.

Region-wise seasonal dependence of EPBs

It is known from the previous section, that the global distribution of the EPBs is spread throughout the different regions of the Earth. In order to have in-detail categorical study, region-wise analysis was performed. The longitudinal extent, which includes America (110°W-20°W), Africa (20°W-70°E), Asia (70°E-160°E) and Pacific (160°E-110°W) are classified as different regional sectors. These longitude sectors are compared to different seasons based on three month intervals around each solstice and equinox. The interpretation of the season and the regions is based on geomagnetic latitude and local time in order to have a comprehensive impressions on the EPB occurrence. Across the American sector, intense level of EPBs are seen across all seasons with maximum occurrence during NDJ (November-December-January) months, but sparse during the June solstice. In the African sector immense number of EPBs are found during the March equinox and June solstice. The scintillation level of EPBs in the Pacific region substantially increases from NDJ months upto ASO (August-September-October) months. Crosswise, the American region has the highest level of EPBs during December solstice. However, across the rest of the seasons, African sector recorded the highest number contributing to the scintillations, but relatively less during the December solstice. On the contrary, the EPBs in the Asian sector are relatively scantly distributed across all seasons, except the March equinox, when compared to the Pacific sector as shown in Fig. 6.

Ann. Geophys. Discuss., https://doi.org/10.5194/angeo-2019-45
Manuscript under review for journal Ann. Geophys.
Discussion started: 25 March 2019

3.3 Altitude variations and solar cycle dependency

In the past, generous amount of research has been conducted in knowing different behavior and characteristics of equatorial plasma bubbles based on ground and in-situ measurements. However, the techniques were incompetent in providing a global altitude resolution. The GPS RO profiles proved favorable in complementing towards plasma irregularity research with a possibility of altitude extent globally. The global coverage combined with the high resolution from the GPS-RO provides comprehensive view of EPBs. Figure 7 illustrates altitude variation of EPBs with respect to latitude on $15\,km \times 5^{\circ}$ grid resolution. The altitude (for the RO profile) is restricted between 150-600 km, since below 150 km lies the E-region and above 600 km, the data is noisy and difficult to extract. Interestingly, during the solar minimum year (2009), the strong scintillation events produced by plasma bubbles are contained between altitude range of 250-300 km. Whereas during the solar maximum, the peak magnitude is culminated between 350-400 km. Because of the quasi-vertical profiles retrieved from the GPS-RO , it can be clearly seen with respect to altitude, that plasma bubbles undergo gradual uplift from solar minimum to solar maximum years. Previous studies with respect to solar cycle demonstrate that increased number of EPBs are detected during the maximum solar activity, whereas number of EPBs shows deterioration during solar minimum years (Xiong et al., 2010; Stolle et al., 2006; Burke et al., 2004). But for the first time, GPS-RO technique was able to provide an insight into bubble variation with respect to altitude. It is understood from the plots, that the occurrence of the high scintillation events resulting from the plasma bubbles displays contraction during solar minimum. Whereas, as we proceed towards solar maximum years, an increase in magnitude of high scintillation events is visible causing it to expand globally.

From the analyses performed in the previous sections, it is known, that the EPBs are highly influenced by the solar cycle. In order to ensure integrity, the high scintillation events are analyzed with the solar sunspot numbers. Figure 8 shows a comparison of solar cycle based on sunspot cycle (Fig. 8a) and relative occurrence numbers of EPBs across different years (Fig. 8b). Figure 8a depicts the current solar sunspot cycle represented by monthly sunspots (blue dots) and a smoothed curve (blue solid line), wherein the least sunspot numbers were observed during 2009, while, maximum solar sunspots were discovered in 2014. Similarly, within Fig. 8b the annual occurrence trend of plasma bubbles is characterized by monthly (red) and smoothed monthly values (green). It is observed that the minimum count of high scintillation events affected by EPBs was during 2009, while the maximum count was noticed during 2014. The manifestation of sunspots number and high scintillation events demonstrated similar occurrence trends for minimum and maximum count, thus displaying a direct link with the solar cycle.

4 Conclusions

In this paper, a nine-year comprehensive study of equatorial plasma bubbles is presented using GPS-RO measurements obtained from the FormoSat-3/COSMIC mission. Around 5 million RO profiles were processed between 2008 and 2016, which covers the solar minimum in 2009 as well as the solar maximum year in 2014. The signals which were undergoing changes due to scintillation caused by plasma bubbles were detected based on amplitude scintillation index known as S4. From the various analyses performed using RO global datasets, we see a striking dependency of the solar cycle on the occurrence of plasma bubbles. Furthermore, the global distribution displays intriguing characteristics of bubbles occurring exclusively along the

Ann. Geophys. Discuss., https://doi.org/10.5194/angeo-2019-45
Manuscript under review for journal Ann. Geophys.
Discussion started: 25 March 2019

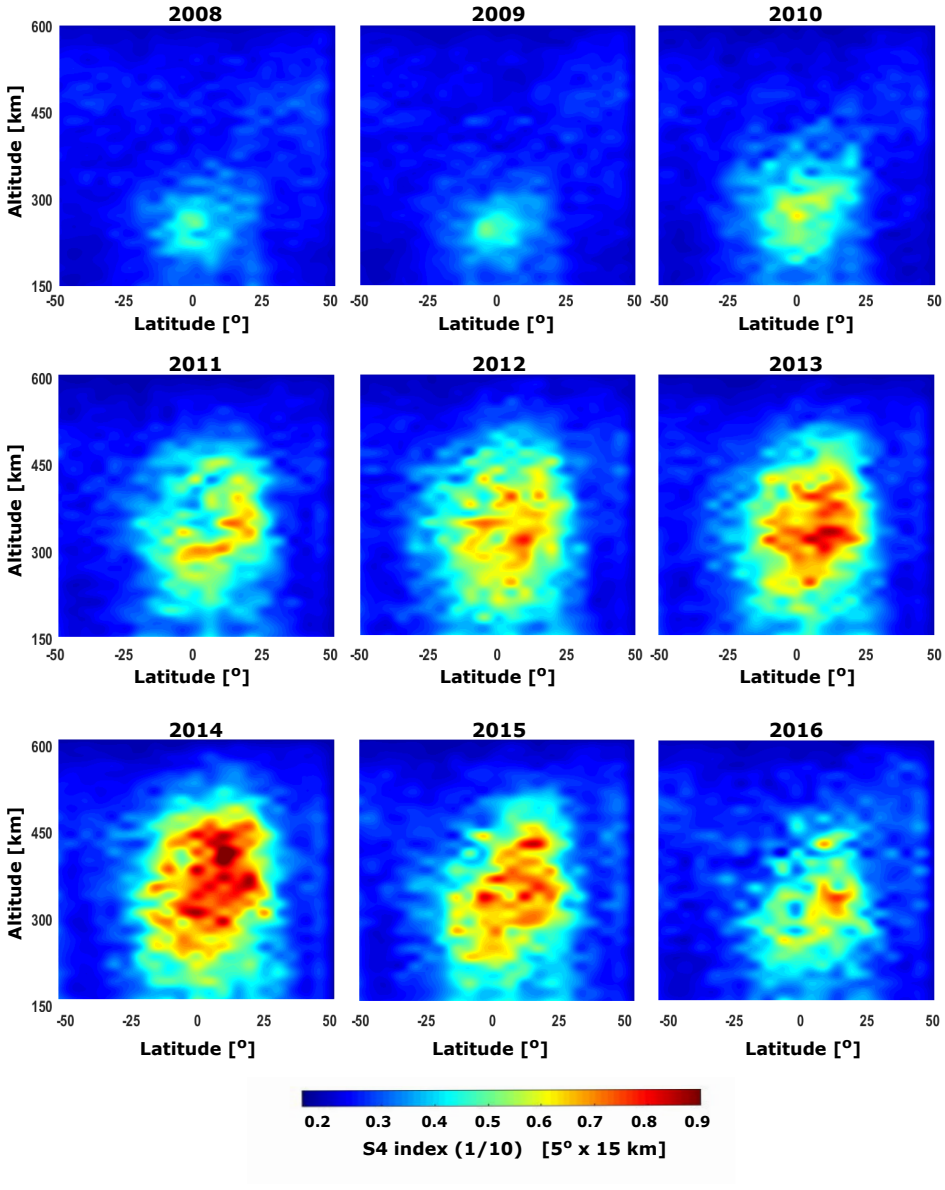

Figure 7. Plot of geographical latitude v/s altitude of EPBs for showing altitude distribution during the years 2007-2016 each based on S4 index values.

geomagnetic equator of the Earth. The rapid depletion of E-layer post sunset cause the development of EPBs with different peak time for the solar maximum and minimum year. In general, the aforementioned results related to the occurrence of plasma bubbles presented in this study, are analogous to the previous studies performed using in-situ as well as ground based measurements. The findings based on the seasonal occurrence mainly explain the dominance of EPBs in the American sector during December solstice and in the African sector during June solstice. In this paper, for the first time a global altitude

Ann. Geophys. Discuss., https://doi.org/10.5194/angeo-2019-45
Manuscript under review for journal Ann. Geophys.
Discussion started: 25 March 2019

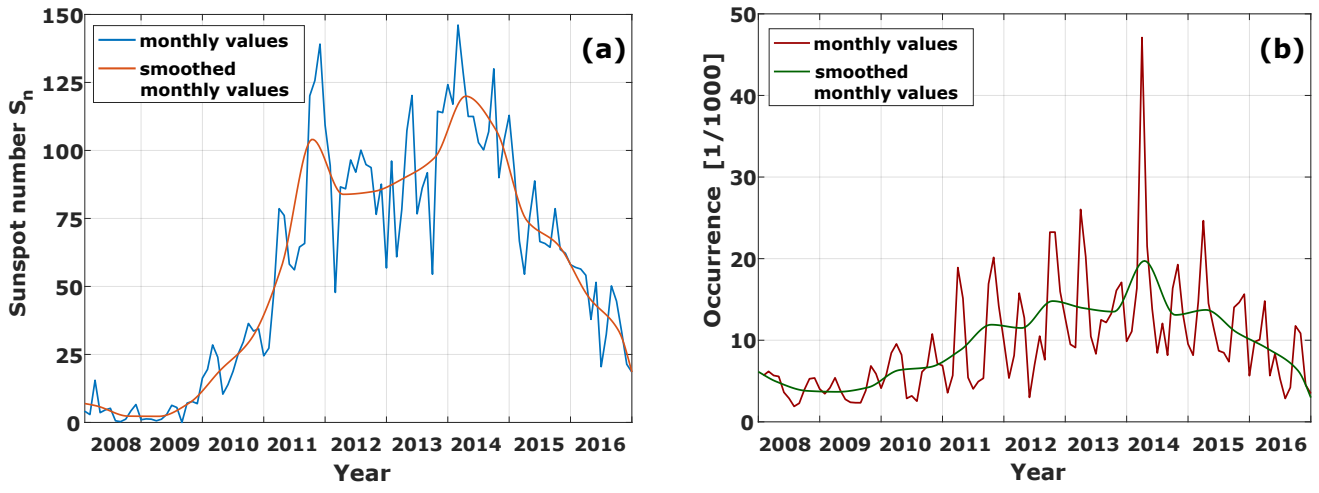

Figure 8. Comparison plot of (a) Sunspot cycle (b) Occurrence trend of EPBs during 2008-2016, having monthly values and smoothed monthly values using low pass filter.

resolution of EPB occurrence is presented. The study reveals the influence of solar cycle, which facilitates the contraction and expansion of plasma bubbles across the complete altitude range.

All in all, GPS-RO proves substantial in providing the climatology of the plasma bubbles phenomenon; but individually, it is not able to provide an introspection of the complete picture of plasma bubbles. This technique could be used as a complementary method along with the well established techniques to study this phenomenon comprehensively. The distinctive interest of using datasets from GPS-RO technique that stands out against its peer techniques for investigating the ionosphere, is due to its high resolution vertical profiles. This allows to have a global perspective of EPB along with a better altitude resolution for investigating such kind of irregularities.

Data availability. Ionospheric radio occultation data is based on FormoSat-3/COSMIC satellite mission available from CDAAC (http://www.cosmic.ucar.edu). The dataset for the solar sunspot number is obtained from Sunspot Index and Long term Solar Observations website (http://www.sidc.be/silso/datafiles)

Ann. Geophys. Discuss., https://doi.org/10.5194/angeo-2019-45
Manuscript under review for journal Ann. Geophys.
Discussion started: 25 March 2019

Annales Geophysicae Discussions
Open Access
EGU

Author contributions. A. Kepkar performed the analysis and drafted the manuscript with the help of C. Arras and J. Wickert. H. Schuh, M. Alizadeh and L.C. Tsai provided with constructive scientific advices.

Competing interests. The authors declare that they have no conflict of interest.

Acknowledgements. The authors recognize the efforts of FormoSat-3/COSMIC team and are grateful for providing the measurements. C. Arras acknowledges the support from Deutsche Forschungsgemeinschaft (DFG) Priority Program DynamicEarth SPP1788. A. Kepkar acknowledges support from DFG under SCHU 1103/15-1.

Ann. Geophys. Discuss., https://doi.org/10.5194/angeo-2019-45
Manuscript under review for journal Ann. Geophys.
Discussion started: 25 March 2019

References

Ahmed, A., Tiwari, R., Ali, S. I., and Jaffer, G.: The Effects of Ionospheric Irregularities on the Navigational Receivers and Its Mitigation, in: International Conference for Emerging Technologies in Computing, pp. 87–97, Springer, 2018.

Anthes, R. A., Bernhardt, P. A., Chen, Y., Cucurull, L., Dymond, K. F., Ector, D., Healy, S. B., Ho, S. P., Hunt, D. C., Kuo, Y. H., Liu, H., Ko, M., McCormick, C., Meehan, T., Randel, W. J., Rocken, C., Schreiner, W. S., Sokolovskiy, S. V., Syndergaard, S., Thompson, D. C., Trenberth, K. E., Wee, T. K., Yen, N. L., and Zeng, Z.: The COSMIC/FORMOSAT-3 mission: Early results, Bulletin of the American Meteorological Society, 89, 313–333, https://doi.org/10.1175/BAMS-89-3-313, 2008.

Arras, C., Wickert, J., Beyerle, G., Heise, S., Schmidt, T., and Jacobi, C.: A global climatology of ionospheric irregularities derived from GPS radio occultation, Geophysical Research Letters, 35, 1–4, 2008.

Arras, C., Jacobi, C., Wickert, J., Heise, S., and Schmidt, T.: Sporadic E signatures revealed from multi-satellite radio occultation measurements, Advances in Radio Science, 8, 225–230, https://doi.org/10.5194/ars-8-225-2010, https://www.adv-radio-sci.net/8/225/2010/, 2010.

Booker, H. and Wells, H.: Scattering of radio waves by the F-region of the ionosphere, Journal of Geophysical Research, 43, 249–256, https://doi.org/10.1029/TE043i00-3p00249, 1938.

Burke, W., Gentile, L., Huang, C., Valladares, C., and Su, S.: Longitudinal variability of equatorial plasma bubbles observed by DMSP and ROCSAT-1, Journal of Geophysical Research: Space Physics, 109, 2004.

Carter, B. A., Zhang, K., Norman, R., Kumar, V. V., and Kumar, S.: On the occurrence of equatorial F-region irregularities during solar minimum using radio occultation measurements, Journal of Geophysical Research: Space Physics, 118, 892–904, https://doi.org/10.1002/jgra.50089, 2013.

Chu, C.-H., Fong, C.-J., Xia-Serafino, W., Shiau, A., Taylor, M., Chang, M.-S., Chen, W.-J., Liu, T.-Y., Liu, N.-C., Martins, B., et al.: An Era of Constellation Observation-FORMOSAT-3/COSMIC and FORMOSAT-7/COSMIC-2, Journal of Aeronautics, Astronautics and Aviation, 50, 335–346, 2018.

Chu, F., Liu, J., Takahashi, H., Sobral, J., Taylor, M., and Medeiros, A.: The climatology of ionospheric plasma bubbles and irregularities over Brazil, in: Annales Geophysicae, vol. 23, pp. 379–384, 2005.

Fejer, B. G. and Kelley, M.: Ionospheric irregularities, Reviews of Geophysics, 18, 401–454, https://doi.org/10.1029/RG018i002p00401, 1980.

Gentile, L., Burke, W., and Rich, F.: A global climatology for equatorial plasma bubbles in the topside ionosphere, in: Annales Geophysicae, vol. 24, pp. 163–172, https://hal.archives-ouvertes.fr/hal-00317925, 2006.

Hanson, W. and Sanatani, S.: Large Ni gradients below the equatorial F peak, Journal of Geophysical Research, 78, 1167–1173, https://doi.org/10.1029/JA078i007p01167, 1973.

Kil, H.: The Morphology of Equatorial Plasma Bubbles - a review, Journal of Astronomy and Space Sciences, 1, 13–19, https://doi.org/10.5140/JASS.2015.32.1.13, 2015.

Kudeki, E. and Bhattacharyya, S.: Postsunset vortex in equatorial F-region plasma drifts and implications for bottomside spread-F, Journal of Geophysical Research: Space Physics, 104, 28 163–28 170, https://doi.org/10.1029/1998JA900111, 1999.

Kursinski, E. R., Hajj, G. A., Schofield, J. T., Linfield, R. P., and Hardy, K. R.: Observing Earth's atmosphere with radio occultation measurements using the Global Positioning System, Journal of Geophysical Research: Atmospheres, 102, 23 429–23 465, https://doi.org/10.1029/97JD01569, 1997.

Lei, J., Syndergaard, S., Burns, A. G., Solomon, S. C., Wang, W., Zeng, Z., Roble, R. G., Wu, Q., Kuo, Y.-H., Holt, J. M., et al.: Comparison of COSMIC ionospheric measurements with ground-based observations and model predictions: Preliminary results, Journal of Geophysical Research: Space Physics, 112, 2007.

McClure, J., Hanson, W., and Hoffman, J.: Plasma bubbles and irregularities in the equatorial ionosphere, Journal of Geophysical Research, 82, 2650–2656, https://doi.org/10.1029/JA082i019p02650, 1977.

Rocken, C., Anthes, R., Exner, M., Hunt, D., Sokolovskiy, S., Ware, R., Gorbunov, M., Schreiner, W., Feng, D., Herman, B., Kuo, Y.-H., and Zou, X.: Analysis and validation of GPS/MET data in the neutral atmosphere, Journal of Geophysical Research: Atmospheres, 102, 29 849–29 866, https://doi.org/10.1029/97JD02400, 1997.

Sahai, Y., Fagundes, P., and Bittencourt, J.: Transequatorial F-region ionospheric plasma bubbles: solar cycle effects, Journal of Atmospheric and Solar-Terrestrial Physics, 62, 1377–1383, https://doi.org/10.1016/S1364-6826(00)00179-6, 2000.

Seif, A., Liu, J.-Y., Mannucci, A. J., Carter, B. A., Norman, R., Caton, R. G., and Tsunoda, R. T.: A Study of Daytime L-Band Scintillation in Association With Sporadic E Along the Magnetic Dip Equator, Radio Science, 2017.

Stolle, C., Lühr, H., Rother, M., and Balasis, G.: Magnetic signatures of equatorial spread F as observed by the CHAMP satellite, Journal of Geophysical Research: Space Physics, 111, https://doi.org/10.1029/2005JA011184, 2006.

Syndergaard, S.: COSMIC S4 Data, COSMIC Data Analysis and Archival Center at UCAR, https://tacc.cwb.gov.tw/cdaac/doc/documents/s4_description.pdf, 2006.

Taori, A., Patra, A., and Joshi, L.: Gravity wave seeding of equatorial plasma bubbles: An investigation with simultaneous F region, E region, and middle atmospheric measurements, Journal of Geophysical Research: Space Physics, 116, https://doi.org/10.1029/2010JA016229, 2011.

Tsai, L.-C., Su, S.-Y., and Liu, C.-H.: Global morphology of ionospheric F-layer scintillations using FS3/COSMIC GPS radio occultation data, GPS Solutions, 21, 1037–1048, https://doi.org/10.1007/s10291-016-0591-4, 2017.

Whalen, J.: Equatorial bubbles observed at the north and south anomaly crests: Dependence on season, local time, and dip latitude, Radio Science, 32, 1559–1566, 1997.

Wickert, J., Beyerle, G., Hajj, G. A., Schwieger, V., and Reigber, C.: GPS radio occultation with CHAMP: Atmospheric profiling utilizing the space-based single difference technique, Geophysical Research Letters, 29, 1–4, https://doi.org/10.1029/2001GL013982, 2002.

Wickert, J., Schmidt, T., Beyerle, G., König, R., Reigber, C., and Jakowski, N.: The radio occultation experiment aboard CHAMP: Operational data analysis and validation of vertical atmospheric profiles, Journal of the Meteorological Society of Japan. Ser. II, 82, 381–395, https://doi.org/10.2151/jmsj.2004.381, 2004.

Wickert, J., Michalak, G., Schmidt, T., Beyerle, G., Cheng, C.-Z., Healy, S. B., Heise, S., Huang, C.-Y., Jakowski, N., Köhler, W., Mayer, C., Offiler, D., Ozawa, E., Pavelyev, A., Rothacher, M., Tapley, B., and Arras, C.: GPS radio occultation: results from CHAMP, GRACE and FORMOSAT-3/COSMIC., Terrestrial, Atmospheric & Oceanic Sciences, 20, 35–50, https://doi.org/: 10.3319/TAO.2007.12.26.01(F3C), 2009.

Woodman, R. F.: Spread F – an old equatorial aeronomy problem finally resolved?, Annales Geophysicae, 27, 1915–1934, https://doi.org/10.5194/angeo-27-1915-2009, 2009.

Woodman, R. F. and La Hoz, C.: Radar observations of F region equatorial irregularities, Journal of Geophysical Research, 81, 5447–5466, https://doi.org/10.1029/JA081i031p05447, 1976.

Xiong, C., Park, J., Lühr, H., Stolle, C., and Ma, S.: Comparing plasma bubble occurrence rates at CHAMP and GRACE altitudes during high and low solar activity, in: Annales Geophysicae, vol. 28, p. 1647, Copernicus GmbH, 2010.

Ann. Geophys. Discuss., https://doi.org/10.5194/angeo-2019-45
Manuscript under review for journal Ann. Geophys.
Discussion started: 25 March 2019

Annales Geophysicae Discussions
Open Access
EGU

Yizengaw, E., Moldwin, M., Mebrahtu, A., Damtie, B., Zesta, E., Valladares, C., and Doherty, P.: Comparison of storm time equatorial ionospheric electrodynamics in the African and American sectors, Journal of Atmospheric and Solar-Terrestrial Physics, 73, 156–163, 2011.

Yizengaw, E., Retterer, J., Pacheco, E., Roddy, P., Groves, K., Caton, R., and Baki, P.: Postmidnight bubbles and scintillations in the quiet-time June solstice, Geophysical Research Letters, 40, 5592–5597, 2013.